On the use of the optimal control theory for deriving wall models for LES

By F. Nicoud[1] AND J. Baggett[2]

1. Motivations and objectives

The large number of grid points required in the near-wall region of attached turbulent boundary layers is the chief obstacle to applying large eddy simulation (LES) to many flows of engineering interest. Current subgrid scale (SGS) models do not accurately model the subgrid scale Reynolds stresses (Baggett *et al.* 1997, Jiménez & Moser 1998). Thus, if the LES is to include the near-wall region, the filter width has to be such that most of the Reynolds stresses are carried by resolved motions. This requires the filter width to scale as a fixed fraction of the local turbulent integral scales which scale as the distance to the wall. Baggett *et al.* (1997) calculated that the number of grid points required for accurate LES of a turbulent boundary layer with a resolved near-wall region scales as $N \sim \mathrm{Re}_\tau^2$, where Re_τ is the friction Reynolds number.

To alleviate these prohibitive near-wall resolution requirements, the no-slip boundary condition is replaced by approximate boundary conditions. The approximate boundary conditions attempt to account for the effects of the unresolved near-wall region on the outer flow. In the most common approach, the wall stresses are modeled and the transpiration velocity is set to zero. This approach was first introduced by Deardorff (1970) and Schumann (1975); the latter assumed the streamwise wall stress was in phase with the streamwise velocity at the first off-wall grid point. More recently, there have been attempts to provide wall stress models that incorporate more physics. For instance, a two-layer approach has been employed in which the three-dimensional unsteady boundary layer equations are integrated on an embedded near-wall grid to estimate the wall stresses (Balaras *et al.* 1996, Cabot 1995). Cabot has shown that the two-layer model can yield better predictions of first-order quantities such as mean wall stress even in complex flow regions such as the separated flow behind a backward-facing step (Cabot 1996). A more complete review is given in Nicoud *et al.* (1999).

However, even the exact wall stresses from a field to which the appropriate LES filter has been applied may not be good approximate boundary conditions for advancing the filtered LES velocity field to the next time step. This is because in LES of a turbulent attached boundary layer in which the first off-wall grid point is in the logarithmic region, the filter width of the LES near the wall is always such that not even the energy-containing eddies can be resolved in the first few grid volumes.

1 Current address: CERFACS, France; nicoud@cerfacs.fr

2 Current address: University of Wisconsin-La Crosse; baggett@math.uwlax.edu

Thus, SGS modeling errors will dominate the near-wall region. The problem of wall stress modeling is inherently coupled to the SGS model used and the numerical resolution. In Nicoud *et al.* (1999), we proposed a strategy for finding wall stress models that accounted for this crucial linkage.

In this note, we review our previous work in which an optimal control strategy was used to find promising new wall stress boundary conditions for coarse LES simulations of turbulent channel flow. We also show how this approach can be extended to the case in which the approximate boundary conditions include both wall stress boundary conditions for the tangential velocities and a transpiration condition on the wall-normal velocity. We begin by describing the general methodology for using a control strategy to explore approximate boundary conditions.

2. General methodology

The information that a wall stress model, or more generally any approximate boundary condition, has to supply to the outer LES is essentially unknown. To overcome this difficulty, we use an optimal control strategy in which the objective is to force the outer LES towards a desired solution by using approximate boundary conditions as control. The optimal strategy does not result in a practical wall model for LES because the solution must already be known, but it does produce reference data that can be used to compare or derive new wall models.

In Nicoud *et al.* (1999), we consider the case in which the control applied to the LES is a wall stress boundary condition with zero wall transpiration velocity. In that case, we use the data from the optimally controlled simulation of turbulent channel flow to derive a practical wall stress model. To do so we approximate by Linear Stochastic Estimation (LSE) the conditional average of the optimal wall stresses given the local velocity field. The resulting LSE wall stress model gives an explicit, algebraic formula relating the wall stresses to the local velocity field at the current time step. The LSE wall model reproduces the results of the optimal control strategy at a cost only slightly higher than LES with no wall model. The LSE wall model, with coefficients fixed once and for all, produces good mean flow predictions for skin-friction Reynolds numbers ranging from 180 to $20,000$ on a 32^3 uniform grid (see section 3.1). Before describing the details of the control strategy and the derivation of a practical model, we summarize the numerical method.

2.1 Numerical method

In this study a second-order accurate finite difference scheme is used to discretize the LES equations on a staggered grid system as proposed by Harlow & Welch, 1965. Given the simple geometry considered (periodic channel flow), more accurate (spectral) methods could have been used. However, these highly accurate methods are not flexible enough to handle industrial applications with complex geometries (e.g. flow around an airfoil), where both low-order numerics for simplicity and wall modeling for high-Reynolds number boundary layers are needed. A staggered grid system is used to avoid the decoupled pressure-velocity mode as well as the prescription of boundary condition for the pressure. The time integration is a third-order Runge-Kutta scheme for all the convection and diffusive terms. The

diffusive terms in the normal direction to the wall are not treated implicitly since only coarse grid computations are considered. Periodic conditions are imposed in the two directions x_1 and x_3 (or x and z) parallel to the walls so that the Poisson equation can be solved efficiently using a FFT-based Poisson solver.

The SGS model is the Smagorinsky model with the coefficient determined by the plane-averaged dynamic procedure proposed by Germano *et al.* (1991). Unless otherwise stated, all quantities are nondimensionalized by the friction velocity, u_τ, and channel half-height, h. The channel walls are at $y = \pm 1$. The skin friction Reynolds number is then defined as $R_\tau = u_\tau h/\nu$. When the mean flow is converged in the statistical sense, the mean streamwise pressure gradient is equal to the wall stress, that is, $-\partial P/\partial x =< \tau_w >= 1$.

Since 'non-resolved' LES are considered in this study, the classical no-slip boundary condition for the velocity components is replaced by a set of approximate boundary conditions. The optimal control problem is written for the case where the two shear stresses τ_{12}^w and τ_{32}^w are provided together with the transpiration velocity v. The sketches in Fig. 1 show the location of the variables and boundary conditions in the staggered grid system. The wall normal direction is x_2 (or y) while u_i (or u, v, w) and P are the velocity components and the pressure. Only the plane (x_1, x_2) is shown.

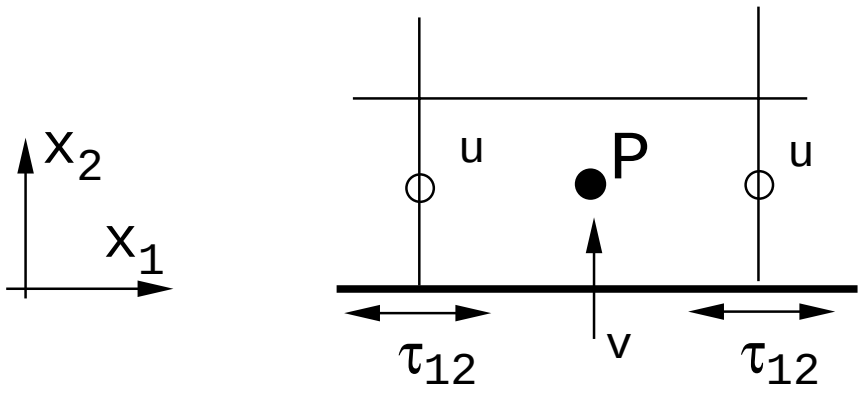

FIGURE 1. Staggered grid system and boundary conditions location.

2.2 Optimal formulation

In the process of deriving a new wall model for LES, it is crucial to keep in mind that:

• The objective is to provide an approximate boundary treatment able to handle very large Reynolds numbers. In this respect, using DNS data as a guide may not be the most judicious choice since these data are only available for low to moderate Reynolds numbers.

• In any coarse grid LES where the first grid point is within the logarithmic region, the turbulent integral length scale ($L \equiv \kappa y$) is less than half the grid spacing ($\Delta y = y$). As a consequence, both subgrid modeling and numerical errors are important. Therefore, the approximate boundary condition should compensate for

these errors if the correct mean profile is to be obtained in a coarse grid computation. In this case the best approximate boundary conditions to supply are not necessarily the physical ones.

It follows that the reference data used to compare or derive new wall models should be obtained from a high Reynolds number LES simulation on a coarse grid. Of course, such a simulation requires a good model for the near-wall region in the first place. The optimal control framework is applied here to conduct such a simulation without *a priori* knowledge of the necessary wall stress boundary conditions. The case of a channel flow with constant pressure gradient is considered. The objective is to optimize the shear stresses τ_{12}^w and τ_{32}^w as well as the transpiration velocity in order to minimize a given cost function. The mathematical formulation detailed in the following subsections is a generalization of the case with zero transpiration velocity presented in Nicoud *et al.* (1999).

2.2.1 State equation

The problem considered is governed by the unsteady, incompressible, filtered Navier-Stokes equations as well as the divergence-free constraint which arises from continuity. The governing equations read:

$$\begin{aligned} \frac{\partial u_i}{\partial t} + \frac{\partial u_i u_j}{\partial x_j} &= -\frac{\partial P}{\partial x_i} + \frac{\partial}{\partial x_j}\left((\nu+\nu_t)\left(\frac{\partial u_i}{\partial x_j}+\frac{\partial u_j}{\partial x_i}\right)\right) \\ \frac{\partial u_j}{\partial x_j} &= 0 \end{aligned} \tag{1}$$

Note that no specific notation is used to describe the spatial filtering associated with the LES formulation. Each variable in the previous and subsequent equations should be understood as a low-pass filtered version of the actual variable (e.g. $u_i \equiv \overline{u_i}$, where the overbar stands for the filtering operator). Equation (1) is valid for any subgrid model based on the Boussinesq assumption. The boundary conditions are:

$$\begin{aligned} \frac{\partial u}{\partial y_n} + \frac{\partial v_n}{\partial x} &= \frac{1}{\nu_w}\phi_u \\ v_n &= \phi_v \\ \frac{\partial w}{\partial y_n} + \frac{\partial w}{\partial z} &= \frac{1}{\nu_w}\phi_w \end{aligned} \tag{2}$$

where the subscript n stands for the outward normal to the wall. Also ν_w is the wall value of the total dynamic viscosity $\nu + \nu_t$. Note that $(\phi_u, \phi_v, \phi_w) = (\tau_{12}^w, v_w, \tau_{32}^w)$ at $y = +1$ and $(\phi_u, \phi_v, \phi_w) = -(\tau_{12}^w, v_w, \tau_{32}^w)$ at $y = -1$ where τ_{12}^w, τ_{32}^w) denote the shear stresses at the wall and v_w is the transpiration velocity.

In the classical optimal control procedure the objective is to reduce the given cost function for some period of time. This method has been proven to be efficient (Abergel & Temam 1990). However, this is a very expensive procedure in terms

of storage and manipulation of many 3D fields over the entire period under consideration. We therefore make use of a more affordable sub-optimal procedure in which the state equation is first discretized in time, then a control procedure is used to minimize the cost function over a short period of time (the time step) at each time step (Bewley *et al.* 1993). This method does not necessarily provide the 'best' answer, but it is much more cost effective than the optimal strategy. The equation of state (1) is, therefore, discretized in time by assuming an implicit discretization:

$$u_i^{n+1} + 2\beta\Delta t \left[\frac{\partial P}{\partial x_i} + \frac{\partial u_i u_j}{\partial x_j} - \frac{\partial}{\partial x_j} \left((\nu + \nu_t) \left(\frac{\partial u_i}{\partial x_j} + \frac{\partial u_j}{\partial x_i} \right) \right) \right]^{n+1} = RHS^n$$
$$-2\beta\Delta t \frac{\partial u_j^{n+1}}{\partial x_j} = 0 \tag{3}$$

The boundary conditions, Eq. (2), apply to Eqs. (3). The terms which depend only on the variables at the previous time step n are gathered in the generic notation RHS^n and disappear in the analytical development (Bewley *et al.* 1993).

2.2.2 Cost function

The goal of the sub-optimal approach is to provide numerical boundary conditions to the flow solver so that the overall solution is consistent with what is expected in a channel flow. In this particular case, the mean velocity profile should be well approximated by a logarithmic profile. Therefore, the cost function is chosen to be a measure at each time step of the difference between the actual mean velocity profile and the target profile $u^+_{\rm ref} = \frac{1}{\kappa} \ln y^+ + C$. This difference can be expressed as:

$$\delta_u(y) = \frac{1}{A} \int \int (u - u_{\rm ref})\, dx\, dz \tag{4}$$

where A stands for the channel area in the homogeneous plane. Note that all the subsequent developments can be done for all forms of the target profile. Noticeably, a more realistic shape could be used in the centerline region. The logarithmic profile is well suited in the 'near wall' region if the grid spacing is large enough so that the first grid point belongs to the log region. In the same way one can define an error in the w mean velocity profile as:

$$\delta_w(y) = \frac{1}{A} \int \int (w - w_{\rm ref})\, dx\, dz \tag{5}$$

where the reference velocity in the z direction is obviously $w_{\rm ref} = 0$ in the present case. A functional of the form :

$$\mathcal{J}(\phi) = \underbrace{\int_{-1}^{+1} \left(\delta_u(y)^2 + \delta_w(y)^2 \right)\, dy}_{\text{Error in mean profiles}} + \frac{\alpha}{A} \underbrace{\int \int_w \left(\phi_u^2 + \phi_v^2 + \phi_w^2 \right)\, dx\, dz}_{\text{Cost}} \tag{6}$$

provides a measure of the difference between the actual and the target mean velocity profiles. The control parameter ϕ is defined as $\phi = (\phi_u, \phi_v, \phi_w)$. A second term quadratic in ϕ and related to the 'cost' of the control is added to build the final cost function to be minimized. It is introduced to avoid the numerical instabilities which would arise if the imposed shear stresses or transpiration velocity become too large during the optimization process. The parameter α is tuned to balance the effects of the two terms in $\mathcal{J}$.

2.2.3 Adjoint problem

The gradient of the cost function $\mathcal{J}$ with respect to the control parameter ϕ is estimated by using the Fréchet differential (Vainberg 1964) defined for any functional $\mathcal{F}$ as:

$$\frac{D\mathcal{F}}{D\phi}\tilde{\phi} = \lim_{\epsilon \to 0} \frac{\mathcal{F}(\phi + \epsilon\tilde{\phi}) - \mathcal{F}(\phi)}{\epsilon} \tag{7}$$

where $\tilde{\phi}$ is an arbitrary direction. From Eq. (6) the derivative of the cost function $\mathcal{J}$ is:

$$\frac{D\mathcal{J}}{D\phi}\tilde{\phi} = \int\int\int_{\Omega} \left[\frac{2\delta_u}{A}\mathcal{U} + \frac{2\delta_w}{A}\mathcal{W} \right] \, dx \, dy \, dz + \frac{2\alpha}{A} \int\int_{w} \phi\tilde{\phi} \, dx \, dz \tag{8}$$

where $\mathcal{U}$ and $\mathcal{W}$ denote the Fréchet derivatives of u and w respectively. Note that in Eq. (8), $\phi\tilde{\phi}$ should be understood as $\phi_u\tilde{\phi}_u + \phi_v\tilde{\phi}_v + \phi_w\tilde{\phi}_w$. An adjoint problem must be formulated to estimate the gradient of $\mathcal{J}$ since the derivatives $\mathcal{U}$ and $\mathcal{W}$ are unknown. The first step is to take the derivative of the semi-discrete state equation (3) to obtain:

$$\begin{aligned} \mathcal{U}_i + 2\beta\Delta t \left[\frac{\partial \mathcal{P}}{\partial x_i} + \mathcal{U}_j \frac{\partial u_i}{\partial x_j} + u_j \frac{\partial \mathcal{U}_i}{\partial x_j} - \frac{\partial}{\partial x_j} \left((\nu + \nu_t) \left(\frac{\partial \mathcal{U}_i}{\partial x_j} + \frac{\partial \mathcal{U}_j}{\partial x_i} \right) \right) \right] &= 0 \\ -2\beta\Delta t \frac{\partial \mathcal{U}_j}{\partial x_j} &= 0 \end{aligned} \tag{9}$$

with the boundary condition:

$$\begin{aligned} \frac{\partial \mathcal{U}}{\partial y_n} + \frac{\partial \mathcal{V}_n}{\partial x} &= \frac{1}{\nu_w}\tilde{\phi_u} \\ \mathcal{V}_n &= \tilde{\phi_v} \\ \frac{\partial \mathcal{W}}{\partial y_n} + \frac{\partial \mathcal{V}_n}{\partial z} &= \frac{1}{\nu_w}\tilde{\phi_w} \end{aligned} \tag{10}$$

The right-hand side term in Eq. (9) is now zero since the flow field at time step n does not depend on the boundary condition to be imposed for the current time step. Therefore, the superscript '$n+1$' has been dropped for clarity. Note also that the Fréchet derivative of the eddy viscosity was supposed to be zero, viz. $D\nu_t/D\phi = 0$,

to obtain Eq. (9). Moreover, this system of equations is linear in the variables $\mathcal{U}_i$ and $\mathcal{P}$, where $\mathcal{P}$ is the Fréchet derivative of pressure. Therefore, it can be written in the form:

$$\mathcal{A}\,\Theta = 0 \tag{11}$$

where $\mathcal{A}$ is a linear operator acting on the vector $\Theta = (\mathcal{U}_i, \mathcal{P})^T$. To bypass the resolution of the differential problem Eq. (11) with unknown boundary conditions equation (10), an adjoint operator $\mathcal{A}^*$ is formulated by considering the equation

$$< \mathcal{A}\,\Theta, \Psi >=< \Theta, \mathcal{A}^*\,\Psi > + \mathrm{BT} \tag{12}$$

where $< a, b >$ stands for the inner product defined as the integral over the volume of the dot product of the two terms a and b and Ψ is the adjoint state vector $\Psi = (\eta_i, \pi)^T$. Practically, the adjoint operator is formed by using successive integrations by parts to turn all the spatial derivatives acting on Θ to derivatives acting on Ψ. Some boundary terms arise during this process which are contained in the term BT of Eq. (12). It is straightforward to show that the adjoint operator $\mathcal{A}^*$ acting on the adjoint state vector Ψ is such that the vector $\mathcal{A}^*\,\Psi$ is defined as:

$$\begin{aligned}\eta_i + 2\beta\Delta t\left[\frac{\partial \pi}{\partial x_i} + \eta_j\frac{\partial u_j}{\partial x_i} - u_j\frac{\partial \eta_i}{\partial x_j} - \frac{\partial}{\partial x_j}\left((\nu+\nu_t)\left(\frac{\partial \eta_i}{\partial x_j}+\frac{\partial \eta_j}{\partial x_i}\right)\right)\right] \\ - 2\beta\Delta t\frac{\partial \eta_j}{\partial x_j}\end{aligned} \tag{13}$$

and that the boundary terms are:

$$\mathrm{BT} = 2\beta\Delta\mathrm{t}\int\int_{\mathrm{w}}(\mathrm{Press} + \mathrm{Conv} + \mathrm{Visc})\ \mathrm{dx}\ \mathrm{dz} \tag{14}$$

with

$$\begin{aligned}\mathrm{Press} &= \mathcal{P}\eta_{2n} \\ \mathrm{Conv} &= \eta_i\mathcal{U}_i v_n \\ \mathrm{Visc} &= -\nu_w\left(\eta_i\frac{\partial \mathcal{U}_i}{\partial y_n} - \mathcal{U}_i\frac{\partial \eta_i}{\partial y_n} + \eta_i\frac{\partial \mathcal{V}_n}{\partial x_i} - \mathcal{U}_i\frac{\partial \eta_{2n}}{\partial x_i}\right)\end{aligned} \tag{15}$$

From Eq. (12), the relation (11) defining the adjoint operator reduces to

$$< \mathcal{A}^*\,\Psi, \Theta >= -\mathrm{BT} \tag{16}$$

2.2.4 Gradient estimate

We now have the liberty to choose boundary condition and right-hand side terms for the adjoint problem such that the relation Eq. (16) can be utilized to compute

the gradient of $\mathcal{J}$. By comparing Eqs. (8), (14), (15), and (16), it appears that a judicious choice for the definition of the adjoint problem is:

$$\mathcal{A}^* \ \Psi = (\frac{2\delta_u}{A}, 0, \frac{2\delta_w}{A}, 0)^T \tag{17}$$

with boundary conditions at the wall:

$$\begin{aligned} \eta_1 v_n + \nu_w \frac{\partial \eta_1}{\partial y_n} &= 0 \\ \eta_{2n} &= 0 \\ \eta_3 v_n + \nu_w \frac{\partial \eta_3}{\partial y_n} &= 0 \end{aligned} \tag{18}$$

In doing so, Eq. (16) can be re-written as

$$\begin{aligned} \frac{D\mathcal{J}}{D\phi}\tilde{\phi} = 2\beta\Delta t \int\int_w \left[\eta_1\tilde{\phi_u} - 2\nu_w \frac{\partial \eta_{2n}}{\partial y_n}\tilde{\phi_v} + \eta_3\tilde{\phi_w}\right] dx\ dz \\ + \frac{2\alpha}{A}\int\int_w \left(\phi_u\tilde{\phi_u} + \phi_v\tilde{\phi_v} + \phi_w\tilde{\phi_w}\right)\ dx\ dz \end{aligned} \tag{19}$$

Since Eq. (19) is valid for all directions $\tilde{\phi}$, the gradient of $\mathcal{J}$ may be extracted:

$$\begin{aligned} \frac{D\mathcal{J}}{D\phi_u} &= 2\beta\Delta t\ \eta_{1,w} + \frac{2\alpha}{A}\phi_u \\ \frac{D\mathcal{J}}{D\phi_v} &= -4\beta\Delta t\ \nu_w\ \left.\frac{\partial \eta_{2n}}{\partial y_n}\right|_w + \frac{2\alpha}{A}\phi_v \\ \frac{D\mathcal{J}}{D\phi_w} &= 2\beta\Delta t\ \eta_{3,w} + \frac{2\alpha}{A}\phi_w \end{aligned} \tag{20}$$

where the subscript w stands for values at the wall. A control procedure using a simple gradient algorithm at each time step may now be proposed such that:

$$\phi^{n+1_{k+1}} = \phi^{n+1_k} - \mu\frac{D\mathcal{J}(\phi^{n+1_k})}{D\phi} \tag{21}$$

Note that the adjoint operator $\mathcal{A}^*$ depends on the state vector $(u_i, P)^T$ at time n+1 so that the state equation and the adjoint problem must be solved simultaneously to obtain the sub-optimal shear stresses and transpiration velocity. More details about the algorithm used to solve the adjoint problem can be found in Nicoud *et al.* (1999).

3. Results

3.1 Case 1: no transpiration

The case without transpiration velocity ($v_n = 0$) has been studied in detail in Nicoud *et al.* (1999). The gradient of the cost function reduces to:

$$\frac{D\mathcal{J}}{D\phi_u} = 2\beta\Delta t\ \eta_{1,w} + \frac{2\alpha}{A}\phi_u$$
$$\frac{D\mathcal{J}}{D\phi_w} = 2\beta\Delta t\ \eta_{3,w} + \frac{2\alpha}{A}\phi_w \tag{22}$$

with the boundary conditions

$$\frac{\partial\eta_1}{\partial y_n} = \eta_{2n} = \frac{\partial\eta_3}{\partial y_n} = 0 \tag{23}$$

for the adjoint problem Eq. (17).

Several LES's have been performed to test the optimal strategy. The grid is uniform in all directions (with typically 32x33x32 cells) and the domain size is $(2\pi h, 2h, 2\pi h/3)$ where h is the channel half height. The Reynolds number based on the friction velocity u_τ and h is 4000 (the range 180-20000 and other mesh resolutions have been investigated in Nicoud *et al.* 1999). Figure 2 shows the mean velocity profile from the coarse LES. The mean value of τ_{12}^w was either provided by the optimal procedure itself or re-computed so that the first point coincides with the logarithmic law $< u >^+ = 2.41 \ln y^+ + 5.2$. The results are very similar in the two cases. The overall agreement is much better than with the shifted model of Piomelli *et al.* (1989). An artificial boundary layer still develops between the second and the third grid point, but its amplitude is much smaller than with the shifted model. The deficit in the log-law intercept is of order 0.25 compared to 1.35 with the explicit, analytical model of Piomelli *et al.*

While the sub-optimal control strategy for generating wall stresses could be used as a wall model for coarse-grid LES, its cost is approximately 20 times greater than of an LES on the same grid compared to an explicit wall stress model such as an analytical model. Furthermore, a target mean velocity profile must be provided to define the objective function. It may be possible to lower the cost of control strategy, but we have not investigated that possibility yet. The real strength of the optimal control strategy is that it yields wall stress boundary conditions that work for coarse-grid, high Reynolds number LES. Thus, a reference data set can be generated against which new wall models can be compared or built. An example of use of such reference data is given in Nicoud *et al.* (1999) where one requires the wall stress model to be the best possible mean square estimate of the sub-optimal wall stress as a function of the velocity field in a neighborhood of the point where the wall stress is required. This is the conditional average of the wall stress given the local velocity field (a conditional average is necessary because the

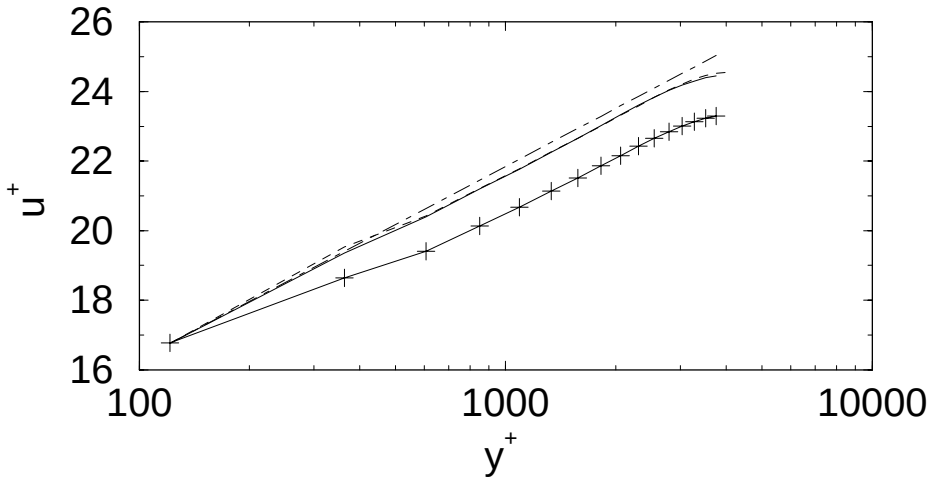

FIGURE 2. Mean velocity profiles for $\mathrm{Re}_\tau = 4000$. ——— : sub-optimal computation; —+— : Shifted model of Piomelli *et al.* (1989); - - - - : LSE model; —·— : $< u >^+ = 2.41 \ln y^+ + 5.2$.

wall stress may have a stochastic, or unpredictable, component with respect to the local velocities). It is denoted by $\langle \tau_{i2}^w(x,z)|\mathbf{E}\rangle$, where $\mathbf{E}$ is a vector of events. In the present study, $\mathbf{E}$ will be a vector containing the local velocity field, but it could easily contain pressure, velocity gradients, quadratic products, or any other quantities which might characterize the wall stresses. The conditional average embodies so much statistical information that it is unlikely that it could be found exactly, but it can be approximated by its LSE, given by (see Adrian *et al.* 1989 for instance):

$$\langle \tau_{i2}^w(x,z)|\mathbf{E}\rangle \approx \check{\tau}_{\mathbf{i2}}^{\mathbf{w}}(\mathbf{x},\mathbf{z}) = \mathbf{L_{ij}E_j} \qquad \mathbf{i = 1,3}, \quad \mathbf{j = 1,2,3},\ldots,\mathbf{N} \tag{24}$$

where N is the number of events being considered and L_{ij} are estimation coefficients relating τ_{i2}^w to E_j. By the statistical orthogonality principle (Papoulis *et al.* 1965), the mean square error between τ_{i2}^w and $\check{\tau}_{i2}^w$ is minimized when the event data are uncorrelated with the error $e_i = \tau_{i2}^w - \check{\tau}_{i2}^w$:

$$\langle e_i E_k\rangle = \langle (\tau_{i2}^w - \check{\tau}_{i2}^w) E_k\rangle = 0. \tag{25}$$

Substituting Eq. (24), the estimation coefficients L_{ij} are governed by:

$$\langle \tau_{i2}^w E_k\rangle = L_{ij}\langle E_j E_k\rangle \tag{26}$$

The matrix $\langle E_j E_k\rangle$ is invertible provided the events are linearly independent. Thus, to obtain the LSE, the correlations $\langle \tau_{i2}^w E_k\rangle$ and $\langle E_j E_k\rangle$ must be found, and the events must be selected that best characterize the wall stress. Though the technique employed here is essentially the same as that of Bagwell *et al.* (1993), the results are different since the reference data used here is already known to work well for a coarse grid LES, whereas Bagwell's reference data comes from a direct numerical

simulation at low Reynolds number. As shown in Nicoud *et al.* (1999), an event field consisting of the nearby velocities is sufficient to yield wall models of the form Eq. (24) that have greater than 80% correlation with the optimal wall stresses. Also shown in Fig. 2 is the mean velocity profile from a simulation with such a LSE model. The new explicit wall model is able to reproduce nearly exactly the results of the sub-optimal simulation.

3.2 Case 2: non zero transpiration

The optimized wall stress boundary conditions in section 3.2 produce a mean velocity profile that is nearly exact for the first two grid points. The small error in the channel interior is believed to be due to the sub-optimal formulation in which the wall stresses are optimized only over each time step. Another reason may be the zero transpiration assumption which is not fully justified in the case of a coarse LES. If we can use the control strategy described above to generate approximate boundary conditions that include nonzero transpiration velocities, then we could use the resulting data to derive new approximate boundary conditions that include transpiration velocities. However, all of the LES's that have been performed with optimized shear stresses and transpiration as control have been found unstable so far. The reason for this failure seems to be in the definition of the boundary conditions for the adjoint problem, Eq. (18).

Consider a typical coarse LES in a channel flow with N^3 grids points (uniform mesh). With second-order differentiation, the Newmann-Dirichlet boundary condition for η_1 may be written as:

$$\eta_{1,g}\left(v_{2n} + \nu_w/\Delta y\right) = \nu_w \eta_1/\Delta y \tag{27}$$

This relates the value of η_1 at the first off-wall point to the ghost value to be imposed in order to satisfy the boundary condition equation (18). In wall units, the standard deviation of the transpiration velocity is expected to be of order unity, with zero mean. Moreover, the term $\nu_w/\Delta y$ is of order 10^-2 (with $R_\tau = O(1000)$ and $N = O(10)$). Thus the term $v_{2n} + \nu_w/\Delta y$ is very close to zero for common values of the transpiration velocity. When this occurs, the boundary condition for the adjoint velocity is ill-posed numerically. Several discretizations of Eq. (18) have been tested to overcome this difficulty but the computations have thus far been unstable.

4. Future plans

Very promising results have been obtained with the sub-optimal procedure in the case where only the shear stresses are optimized. The control procedure provided reference data to derive a new, practical wall stress model. In the case which includes a nonzero transpiration velocity, the classic set of boundary conditions for the LES equations (two shear stresses and normal velocity) leads to a sub-optimal formulation that is well defined mathematically but ill-posed numerically. To overcome this difficulty, a simple way may be to use a weak formulation to prescribe the condition equation (18).

The next step along these lines is to investigate so-called "off-wall" approximate conditions. In this approach, which has met with limited success thus far (see Baggett 1997, Jiménez & Vasco 1998, Nicoud *et al.* 1998), the approximate boundary condition is used to provide Dirichlet boundary conditions directly to the LES velocity field at some point away from the wall where the LES filter width is sufficiently small so that the LES computation is known to be reliable. The sub-optimal control strategy may be useful in determining if such an approach is at all feasible. If so, the control strategy can provide reference data for deriving a practical set of off-wall boundary conditions.

REFERENCES

Abergel, F. & Temam, R. 1990 On some control problems in fluid mechanics. *Theoret. Comput. Fluid Dyn.* **1,** 303-325.

Adrian, R. J., Jones, B. G., Chung, M. K., Hassan, Y., Nithianandan, C. K. & Tung, A. 1989 Approximation of turbulent conditional averages by stochastic estimation. *Phys. Fluids.* **1,** 992-998.

Baggett, J. S. 1997 Some modeling requirements for wall models in large eddy simulation. *Annual Research Briefs.* Center for Turbulence Research, NASA/Stanford Univ. 123-134.

Baggett, J. S., Jiménez, J. & Kravchenko, A. G. 1997 Resolution requirements in large-eddy simulations of shear flows. *Annual Research Briefs.* Center for Turbulence Research, NASA/Stanford Univ. 51-66.

Bagwell, T. G., Adrian, R. J., Moser, R. D. & Kim, J. 1993 Improved approximation of wall shear stress boundary conditions for large eddy simulation. *Near-Wall Turbulent Flows,* Elsevier Science Publishers. So, R. M. C., Speziale, C. B. and Launder, B. E., Eds.

Balaras, E., Benocci, C. & Piomelli, U. 1996 Two-layer approximate boundary conditions for large-eddy simulations. *AIAA J.* **34,** 1111-1119.

Bewley, T., Choi, H., Temam, R. & Moin, P. 1993 Optimal feedback control of turbulent channel flow. *Annual Research Briefs.* Center for Turbulence Research, NASA/Stanford Univ. 3-14.

Cabot, W. 1995 Large-eddy simulations with wall models. *Annual Research Briefs.* Center for Turbulence Research, NASA/Stanford Univ. 41-50.

Cabot, W. 1996 Near-wall models in large eddy simulations of flow behind a backward-facing step. *Annual Research Briefs.* Center for Turbulence Research, NASA/Stanford Univ. 199-210.

Deardorff, J. W. 1970 A numerical study of three-dimensional turbulent channel flow at large Reynolds numbers. *J. Fluid Mech.* **41,** 453-480.

Germano, M., Piomelli, U., Moin, P. & Cabot, W. 1991 A dynamic subgrid-scale eddy viscosity model. *Phys. Fluids.* **3,** 1760-1765.

Harlow, F. H. & Welch, J. E. 1965 Numerical calculation of time-dependent viscous incompressible flow of fluid with free surface. *Phys. Fluids.* **8,** 2182-2189.

Jiménez, J. & Moser, R. D. 1998 LES: Where we are and what we can expect. *AIAA 98-2891.*

Jiménez, J. & Vasco, C. 1998 Approximate lateral boundary conditions for turbulent simulations. *Proceedings of the Summer Program.* Center for Turbulence Research, NASA/Stanford Univ. 399-412.

Nicoud, F., Winckelmans, G., Carati, D., Baggett, J. & Cabot, W. 1998 Boundary condition for LES away from the wall. *Proceedings of the Summer Program.* Center for Turbulence Research, NASA/Stanford Univ. 413-422.

Nicoud, F., Baggett, J., Moin, P. & Cabot, W. 1999 LES Wall-modeling based on optimal control theory. *Phys. Fluids.* Submitted.

Papoulis, A. 1965 *Probability, Random Variables, and Stochastic Processes.* New York: McGraw Hill.

Piomelli, U., Ferziger, J., Moin, P. & Kim, J. 1989 New approximate boundary conditions for large eddy simulations of wall-bounded flows. *Phys. Fluids.* **1,** 1061-1068.

Schumann, U. 1975 Subgrid scale model for finite difference simulations of turbulent flows in plane channels and annuli. *J. Comp. Phys.* **18,** 376-404.

Vainberg, M. 1964 *Variational methods for the study of nonlinear operators.* Holden-Day.